Identification of Damage Location using a Novel Substructure-Based Frequency Response Function Approach with an Imote2.NET-Based Wireless System

T.H. Lin
Sinotech Engineering Consultants, Inc., Taiwan (R.O.C.)

S.L. Hung & C.S. Huang
National Chiao Tung University, Taiwan (R.O.C.)

T.K. Lin
National Center for Research on Earthquake Engineering, Taiwan (R.O.C.)

15 WCEE
LISBOA 2012

SUMMARY
This work located damage to building structures subjected to earthquake excitation using a novel substructure-based FRF approach with a damage location index (*SubFRFDI*). An Imote2-based wireless structural health monitoring system was also developed and employed in experimental studies due to its many benefits, such as deployment flexibility, low maintenance cost, low power consumption, self-organization capability, and wireless communication capability. The feasibility and robustness of the proposed Imote2.NET-based wireless structural health monitoring system were assessed using a 1/8-scale three-storey steel-frame model. Following, the proposed *SubFRFDI* was further applied to identify damage locations in an experimental 1/4-scale six-storey steel structure with the proposed Imote2.NET-based wireless structural health monitoring system. In the experimental study, the proposed *SubFRFDI* identified damage locations conveniently and accurately.

Keywords: Structural Health Monitoring (SHM), FRF, Wireless Sensor Networks

1. INTRODUCTION

A building structure may sustain damage either when subjected to severe loading like a strong earthquake or when its material deteriorates. Hence, monitoring the structural health of buildings and civil infrastructure has received considerable interest in the last decade. Monitoring the structural health of a given structural system is a damage identification process that includes damage detection, damage localization, damage type evaluation, and damage severity estimation. Damage can be defined as changes to a structural system, such as its material and/or geometric properties, that alter its current or future performance (Worden et al. 2008; Sohn et al. 2004).

A frequency response function (FRF) expresses the structural response to an applied force as a function of frequency. This response may be represented in terms of displacement, velocity, or acceleration (Cauberghe et al. 2004; Celic and Boltezar 2008). Theoretically, FRF can be expressed in terms of system properties of mass, stiffness, damping, and modal properties. Accordingly, an FRF scheme is reasonably expected to be feasible for detecting structural damage.

Several studies have applied the FRF to locate damage. Thyagarajan et al. (1998) developed a method based on FRF data and an optimal number of sensors on a structure to identify damage locations, overcoming the former limitation of large number of computations required for high dof. structure. Lee and Shin (2002) combined an FRF-based structural damage identification method (SDIM) with a reduced domain approach to detect damage to beam structures. Other investigations have extended FRF methods to improve the detection of damage locations. Sampaio et al. (1999) developed a theoretical FRF curvature method and evaluated the efficiency of this method using numerically simulated data and experimental data for a real bridge. Maia et al. (2003) also presented an FRF curvature-based damage detection method and compared its performance with that of a conventional mode shape-based method. Liu et al. (2009) developed an FRF shape-based method.

This method utilized the imaginary parts of FRF shapes of a beam structure to identify the damage location before and after damage. FRF have also been applied to detect damage in a building structure. By using measured FRF and neural networks (NNs), Ni et al. (2006) identified the seismic damage of a 38-storey building model. Furukawa et al. (2006) developed a damage detection method using uncertain FRFs based on a statistical bootstrap method and then applied it to a building structure. Kanwar et al. (2008) demonstrated the feasibility of using FRF to the structural damage of reinforced concrete buildings. By using FRF, Hsu and Loh (2009) detected damage of building structure subjected to earthquake ground excitation.

Dense distributed sensors are essential to increasing efficiency of FRF-based damage identification method. Characterized by its low manufacturing costs, low power requirements, miniaturized size, and no need for cabling, the wireless sensor networks (WSN) is an attractive sensing technology for deploying dense distributed sensors (Lynch and Loh 2006; Spencer et al. 2004). The MICA mote is a commercially available product that has been used extensively by researchers and developers. However, Mica motes have certain limitations, including limited sampling rate, processing ability, storage, and transmission ability. Therefore, the advanced wireless sensor platform Imote2 is widely considered an adequate choice for developing and deploying customized wireless sensor networks efficiently (Nagayama et al. 2009; Rice et al. 2010). This work presents an easy-to-use development environment based on the .NET Micro Framework. Applications can be implemented efficiently under the .NET Micro Framework. This accelerated development of SHM applications demonstrates the importance of the user-friendly development environment. An Imote2.NET-based wireless SHM system was developed and employed in experimental studies.

This work has two primary purposes. First, a novel substructure-based FRF approach with a damage location index (*SubFRFDI*) was proposed to localize damage to building structures from seismic response data. Second, a wireless SHM system was developed based on Imote2.NET, which is an advanced sensor platform compatible with .NET Micro Framework. The feasibility and robustness of the proposed Imote2.NET-based wireless SHM system were assessed using a 1/8-scale three-storey steel-frame model. This work then designed a 1/4-scale six-storey steel frame and experimentally generated different damage scenarios by subjecting this structure various base excitations via shaking table tests. An Imote2-based wireless SHM system was employed for data sensing, logging, storing, processing and analyzing. Finally, this work applied the proposed damage detection approach to process measured data from the wireless sensing system to detect damage locations under different damage scenarios.

2. SUBSTRUCTURE-BASED FRF APPROACH FOR DAMAGE LOCATION DETECTION

In a shear building, beams and floor systems are assumed to be rigid in flexure. Several factors, such as the axial deformation of beams and columns, and the effect of axial force on column stiffness, are neglected in analysis. Although an ideal shear building does not exist in practice, it is helpful for illustrating the use of substructure-based FRF to locate damage. For a damped multi-degree of freedom (MDOF) shear building with, say, N dofs., the equations of motion are

$$[M]\{\ddot{x}(t)\} + [C]\{\dot{x}(t)\} + [K]\{x(t)\} = \{f(t)\} \tag{2.1}$$

where $[M], [C]$, and $[K]$ are $N \times N$ mass, viscous damping, and stiffness matrices, respectively; and $x(t)$ and $f(t)$ are $N \times 1$ vectors of the displacement functions and effective external excitation load, respectively. The mass matrix is diagonal, while $[C]$ and $[K]$ are tri-diagonal. Applying the Fourier transform to Eq. (2.1) and performing a simple arrangement yield and can be written simply as

$$\{X\} = [H(\omega)]\{F\} \tag{2.2}$$

where $[H(\omega)]$ is an FRF of the system and equals $([K]+i\omega[C]-\omega^2[M])^{-1}$.

The MDOF structure is divided herein into various substructures. Consider an N-storey shear building subjected to base excitations with acceleration a_g, which can be described by a simplified model (Fig. 1). N substructures of the original structure can be easily established. The first substructure has the 1st—N^{th} dofs. while the second has the 2nd—N^{th} dofs. Accordingly, the ith substructure has the ith—N^{th} dofs. (Fig. 1). The responses of any degrees of freedom of the ith substructure are the same as those of the original complete structure.
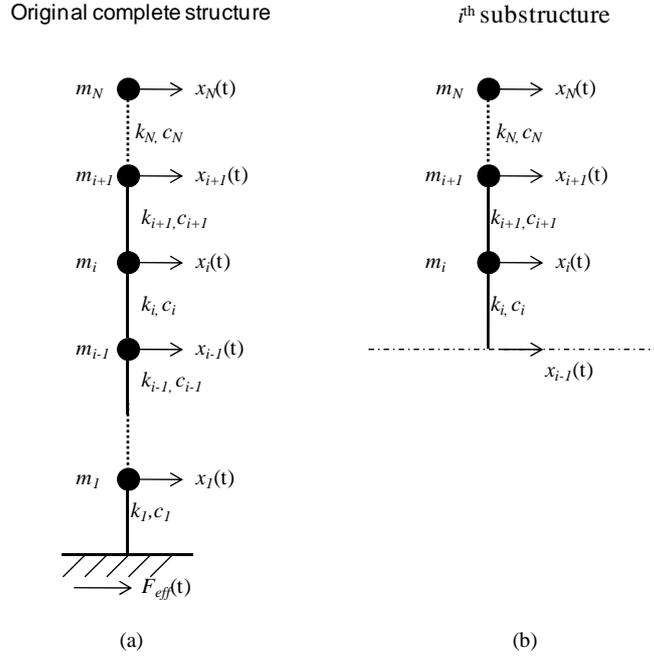

Figure 1. (a) Original complete structure, (b) the ith substructure.

When $i \neq 1$, the equations of motion of the ith substructure can be expressed as

$$
\begin{bmatrix} m_i & \cdots & \cdots & 0 \\ \vdots & m_{i+1} & & \vdots \\ \vdots & & \ddots & \vdots \\ 0 & \cdots & \cdots & m_N \end{bmatrix} \begin{Bmatrix} \ddot{\tilde{x}}_i(t) \\ \ddot{\tilde{x}}_{i+1}(t) \\ \vdots \\ \ddot{\tilde{x}}_N(t) \end{Bmatrix} + \begin{bmatrix} c_i+c_{i+1} & -c_{i+1} & & \\ -c_{i+1} & c_{i+1}+c_{i+2} & -c_{i+2} & \cdots & 0 \\ & \vdots & & \ddots & \vdots \\ & 0 & & \cdots & c_N \end{bmatrix} \begin{Bmatrix} \dot{\tilde{x}}_i(t) \\ \dot{\tilde{x}}_{i+1}(t) \\ \vdots \\ \dot{\tilde{x}}_N(t) \end{Bmatrix} +
$$

$$
\begin{bmatrix} k_i+k_{i+1} & -k_{i+1} & & \\ -k_{i+1} & k_{i+1}+k_{i+2} & -k_{i+2} & \cdots & 0 \\ & \vdots & & \ddots & \vdots \\ & 0 & & \cdots & k_N \end{bmatrix} \begin{Bmatrix} \tilde{x}_i(t) \\ \tilde{x}_{i+1}(t) \\ \vdots \\ \tilde{x}_N(t) \end{Bmatrix} = \begin{Bmatrix} c_i\dot{\tilde{x}}_{i-1}(t)+k_i\tilde{x}_{i-1}(t) \\ 0 \\ \vdots \\ 0 \end{Bmatrix}
$$

(2.3)

where $\tilde{x}_i(t)$ is the total displacement response of the ith dof., and $\ddot{\tilde{x}}_i(t)=\ddot{x}(t)+a_g$. Equation (2.3) represents a single input/multiple output system. Clearly, the substructure-based FRFs of the jth dof. in the ith substructure are

$$
H_j^{(i)}(\omega)=\frac{\tilde{X}_j}{(i\omega c_i+k_i)\tilde{X}_{i-1}} \quad , \quad j=i \text{ to } N
$$

(2.4)

where $\tilde{X}_j$ and $\tilde{X}_{i-1}$ are the Fourier transforms of $\tilde{x}_j(t)$ and $\tilde{x}_{i-1}(t)$, respectively. The substructure-based FRF given by Eq. (2.4) depends on the properties of the ith—N^{th} dofs. To estimate $H_j^{(i)}(\omega)$ from Eq. (2.4), c_i and k_i must be known. Unfortunately, c_i and k_i are usually unknown in the damage diagnosis process. Moreover, acceleration responses are normally measured in monitoring the responses of a structure in an earthquake. Therefore, the measured acceleration responses of the original complete structure are used herein and these substructure-based FRFs are further simplified as

$$\tilde{H}_j^{(i)}(\omega) = \frac{\ddot{\tilde{X}}_j}{\ddot{\tilde{X}}_{i-1}}, \quad j = i \text{ to } N \tag{2.5}$$

where $\ddot{\tilde{X}}_j$ and $\ddot{\tilde{X}}_{i-1}$ are the Fourier transforms of $\ddot{\tilde{x}}_j(t)$ and $\ddot{\tilde{x}}_{i-1}(t)$, respectively. A specified substructure-based FRF, $H_j^{(i)}(\omega)$, can be estimated from measured acceleration of the $(i-1)^{\text{th}}$ and j^{th} dofs. Notably, when $i = 1$, referring to the original complete structural system, these substructure-based FRFs are given by

$$\tilde{H}_j^{(1)}(\omega) = \frac{\ddot{\tilde{X}}_j}{A_g}, \quad j = 1 \text{ to } N \tag{2.6}$$

where A_g is the Fourier transform of a_g.

Theoretically, when the damage is assumed to have occurred in the column(s) between the ith and $(i-1)^{\text{th}}$ dofs. (such that k_i is reduced *and* c_i is increased), the substructure-based FRF is significantly altered in the ith dof., as described by, $\tilde{H}_i^{(i)}(\omega)$. Likewise, if stiffness k_i and k_l decline simultaneously, then the change in the corresponding FRFs, $\tilde{H}_i^{(i)}(\omega)$ and $\tilde{H}_l^{(l)}(\omega)$, is greater than what would typically be observed in $\tilde{H}_j^{(i)}(\omega)$. Consequently, damage can be identified as having occurred at a single or multiple sites. For efficiency, only one substructure-based FRF, $\tilde{H}_i^{(i)}(\omega)$, is determined herein for each substructure to reduce the computational time. Damage of the shearing building structures is located based on the FRFs, $\tilde{H}_1^{(1)}(\omega)$, $\tilde{H}_2^{(2)}(\omega)$, ..., $\tilde{H}_N^{(N)}(\omega)$, of all substructures.

Based on the aforementioned description, change in the substructure-based FRF is related to damage and can be utilized as an essential index to locate damage of the building structures. The operating conditions of this work are based on a known initial state, continuously measured seismic response data, and comparisons of before-and-after damage scenario for a shear building. Initially, sensors are deployed on the shear building and the corresponding response data are measured immediately after an earthquake excitation. The initial stiffness of the structure is then defined and the corresponding FRFs $\tilde{H}_{1,u}^{(1)}(\omega), \tilde{H}_{2,u}^{(2)}(\omega)$ ..., $\tilde{H}_{N,u}^{(N)}(\omega)$ are computed as a known undamaged state, also referred to as a before-scenario state. Next, the sensors continuously collect seismic response data of the structure after each subsequent earthquake and the particular FRFs $\tilde{H}_{1,d}^{(1)}(\omega), \tilde{H}_{2,d}^{(2)}(\omega)$ ..., $\tilde{H}_{N,d}^{(N)}(\omega)$ are obtained following, referred to as an after-scenario state. Before and after damage scenarios are compared to determine the damage location since a change in the substructure-based FRF is related to damage. A *dissimilarity* between the substructure-based FRFs in damaged and undamaged states can be used to identify the damage. The absolute dissimilarity $\bar{P}_i(\omega)$ is defined as

$$\bar{P}_i(\omega) = \left\| \left| \tilde{H}_{i,d}^{(i)}(\omega) \right| - \left| \tilde{H}_{i,u}^{(i)}(\omega) \right| \right\| \tag{2.7}$$

where $\left|\tilde{H}_{i,d}^{(i)}(\omega)\right|$ and $\left|\tilde{H}_{i,u}^{(i)}(\omega)\right|$ are the magnitudes of $\tilde{H}_i^{(i)}$ in the damaged and undamaged states, respectively. These N *dissimilarities* $\bar{P}_1(\omega) - \bar{P}_N(\omega)$ can be correspondingly calculated for a shear building with N floors. To locate conveniently and quantify the damage, a substructure-based FRF damage location index (*SubFRFDI*) for the ith substructure is proposed. It is given by

$$SubFRFDI_i = 1 - Exp\left[-\rho^2\left(\sum_{\omega=a}^{b}\left\{\left(NDF_i(\omega)\right)^2\right\}\right)/n\right] \tag{2.8}$$

where ρ, a, b, and n are working parameters and the $NDF_i(\omega)$ is expressed as

$$NDF_i(\omega) = \frac{\bar{P}_i(\omega)}{\max\left[\left|\tilde{H}_{i,d}^{(i)}(\omega)\right|_{max}, \left|\tilde{H}_{i,u}^{(i)}(\omega)\right|_{max}\right]} \tag{2.9}$$

The coefficient ρ is a control value that scales the index between zero and one and is set to five in this work. The range of selected frequencies for calculating *SubFRFDI* is set to a—b, where a is a starting frequency of zero and b is the end frequency, which equals the first modal frequency (undamaged state). The aforesaid a and b are determined by trial-and-error method. The value n equals $(b - a)$ divided by sampling time, which is 0.005 s in this work.

If the properties of a structural system do not change, then the $SubFRFDI_i$ is close to zero. However, if the damage to storey i in a shear building is severe, then the value of $SubFRFDI_i$ is high. The resulting apparently significant peak value(s) of *SubFRFDI* indicate(s) that damage occurs at either a single site or at multiple sites. For instance, if damage occurs only in the ith dof., then only the $SubFRFDI_i$ from all *SubFRFDI* has a significant peak value. If damage occurs at more than one site, such as in the ith, j^{th}, and k^{th} dofs., then the corresponding *SubFRFDIs* will all have significant peak values.

3. DEVELOPMENT OF IMOTE2.NET BASED WIRELESS SHM SYSTEM

Figure 2 schematically depicts the proposed Imote2.NET based wireless SHM system architecture. The proposed architecture comprises hardware and software systems. The proposed software system of Imote2.NET-based wireless SHM system is a three-tier framework, i.e. node, logging and processing tiers.

The proposed reliable data-sensing and transmission protocol between the sensing nodes and base station are presented. First, after sensing nodes and base station are initialized, the base station sends an inquiring packet to confirm whether the sending nodes are ready. The sending nodes and base station then exchange timestamp packets to synchronize together based on a two-phase synchronization scheme (Syed and Heidemann 2006). In general, two main clock errors must be corrected, i.e. skew and offset. During the first phase, the proposed protocol models the skew of all sensing node's clock; each node is then skew synchronized. Next, the skew is estimated by performing linear regression over multiple timestamp packets from the base station. Each timestamp packet P_i contains the transmit timestamp $t_{B,i}$ obtained at the MAC level, just before the packet leaves the base station. Sensing nodes receive this packet at absolute time $t_{B,i} + D_{B \rightarrow S}$ where $D_{B \rightarrow S}$ refers to the unknown propagation delay between the base station and the sensing nodes. The sensing nodes then record their local time $LT_S(t_{B,i} + D_{B \rightarrow S})$. Although this local time includes error due to clock skew and offset in addition to propagation delay, the skew of the local clock can still be modeled with respect to reference clock of the base station by performing linear regression on the difference between $t_{B,i}$ and

$LT_S(t_{B,i} + D_{B\to S})$. For N packets, the clock skew can be modeled by linear regression over the data set of (x_i, y_i) pairs, where x_i and y_i are $(t_{B,i} - LT_S(t_{B,i} + D_{B\to S}))$ and $LT_S(t_{B,i} + D_{B\to S})$, respectively.
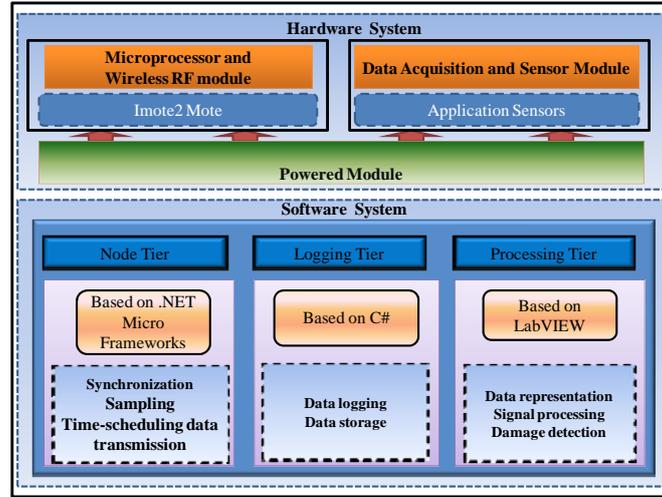

Figure 2. Architecture of Imote2.NET-based wireless SHM system.

During the second phase, the clock offset is corrected by the classical two-way synchronization exchange in a manner similar that of the TPSN synchronization protocol (Ganeriwal et al. 2003). Once obtaining a sufficient number of packets to estimate the skew, the sensing nodes send a packet with the skew-corrected local timestamp, $T1 = LT'_S(T1)$, to the base station. The base station records its received local time $T2 = LT_B(T1 + D_{S\to B})$, then replies with a packet to sensing nodes with $T2$ and transmit timestamp $T3$. Once receiving the packet, the sensing nodes record the skew-corrected local time $T4 = LT'_S(T3 + D_{B\to S})$. Finally, the sensing node can compute its clock offset, $T4$, as the formula $((T2\text{-}T1) - (T4\text{-}T3))/2$.

Following completion of the synchronization, the sampling procedure for all sensing nodes starts simply by performing sampling data and writing data to an array. The corresponding parameters, such as sampling rate, data type, and data length, are declared before the sampling start. Following the sampling, the time-scheduling data transmission procedure is initiated to send data from the sensing nodes to the base station. Initially, the sensing nodes wait until a *sending-delay* time is equivalent to (*total sampling time + total packet sending time*)* (*node ID*). For instance, if the *node ID* is 0, the sensing node 0 transmits packet immediately since the *sending-delay* equals zero. The data in each sensing node are then taken from the array, filled in a packet, and sent to the base station. Based on this procedure, each node sequentially sends the data to the base station with a respective *sending-delay*, which can avoid the packet collision. However, packets losses occur occasionally, even when the time-scheduling data transmission can avoid packets collision. The base station thus continuously checks the number of packets in sequences from the sensing nodes and records the number of each missing packet in the sequence. Therefore, the base station can request a sensor node to rectify missed packets.

Herein, the node tier consists of developed application functions and is installed on all sensor nodes and a base station node. The logging tier, implemented based on C#, is installed only on the base station and is intended for logging data and data storage. A processing tier is implemented on a PC connected to a base station. The processing tier is developed using LabVIEW. This tier has several functions. First, the raw data is converted into engineering unit and then stored in a database. Next, a customized user interface can represent the data by selecting the desired sensor node. The sensing data can also be analyzed by an advanced signal processing tool, e.g., filtering, smoothing, denoise, FFT, wavelet, and further data analysis. Finally, the above mentioned novel substructure-based FRF approach with a damage location index is implemented in this tier to locate the structural damage.

After each node is installed with abovementioned software, the Imote2.NET based wireless sensor network is constructed and deployed on a 1/8-scaled three-storey steel frame model to demonstrate the feasibility and robustness of the Imote2.NET-based wireless SHM system. For structural dynamic response measuring, wireless sensing nodes were deployed at the center of each floor of the 1/8-scaled steel frame model. A conventional wired sensing system was also set on the center of each floor for reference purposes. The steel frame model was excited using earthquake time history excitation data by the Quanser shaking table. Measured structural dynamic responses were collected via sensing nodes and sent to the base station connected to a host PC for data acquisition. Acceleration measurements from the wireless sensors identified natural frequencies by applying ANN-based system identification model (ANNSI) (Wen et al. 2007). The corresponding first three natural frequencies of the structure were 1.83, 5.42, and 7.96Hz. The modal assurance criterion (MAC) was defined as a degree of consistency between one model and another reference modal (Allemang 2003). In this test, the MAC value was 1 means that the modal parameters can be considered reasonable.

4. APPLICATION TO EXPERIMENTAL RESPONSES MEASURED BY A IMOTE2.NET-BASED WIRELESS SHM SYSTEM

The Imote2.NET-based wireless SHM system was developed and employed experimentally. The Imote2.NET-based sensing nodes were deployed on a steel frame model to monitor health status. The experimental model was a 1/4-scale six-storey steel structure that was designed by the National Center for Research on Earthquake Engineering (NCREE), Taiwan. Figure 3 shows a photograph of the test structure. The floors, beams, and columns were connected using bolts. Various measurement sensors, including 3-axes accelerometers, an LVDT, and velocity sensors, were deployed. Simultaneously, the Imote2.NET-based wireless SHM system was deployed for sensing, logging, storing, processing, and analyzing thus obtained (Fig. 3). Four damage scenarios were considered to simulate states of damage to the steel frame model. All experiments involved excitation using a 100 gal El Centro earthquake input on a shaking table at NCREE. Table 1 present the four prescribed damage scenarios.

Table 1. Description damage scenarios for the steel-frame model.

Damage scenario case	Description
Damage scenario 1	Reduced 3.75 cm width in the medium height of each column at 1st floor.
Damage scenario 2	Reduced 7.5 cm width in the medium height of each column at 1st floor.
Damage scenario 3	Reduced 7.5 cm width and 6mm thickness in the medium height of each column at 1st floor.
Damage scenario 4	Reduced 12 cm width in the medium height of each column at 3rd floor.

In this experiment, the Imote2.NET-based sensing nodes with reliable data-sensing and transmission protocol were deployed on each floor and the shaking table. The measurement period was 60 s, during which data were sampled at 200 Hz. This reliable data-sensing and transmission protocol provided excellent data sensing and transmission quality for determining dynamic structural properties. Based on steel frame responses, the modal properties were identified using system identification procedures. Table 2 compares modal parameters identified using the ANN-based system identification approach (Huang et al. 2003) with the measured data obtained by Imote2.NET-based sensing nodes and conventional sensors. Comparisons demonstrate that data obtained using the Imote2 sensor nodes can be utilized reasonably to calculate modal parameters, confirming the good quality of data collection using the wireless sensing system.
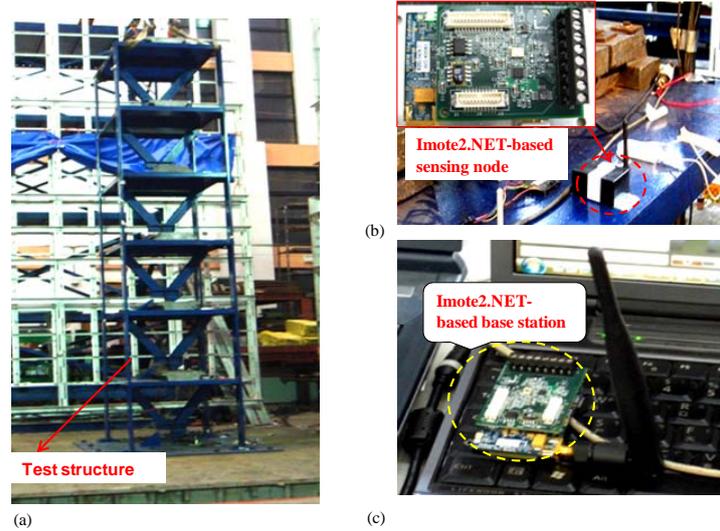
Figure 3. (a) A photograph of the test structure. (b) The Imote2.NET-based sensing nodes fixed on the floor. (c) The Imote2.NET-based wireless data collection base station.

Table 2. Comparisons of modal parameters identified by Imote2 sensor nodes and conventional sensors.

	Frequency (Hz)			Damping (%)		
Mode	Imote2	Conventional sensor	RMSE	Imote2	Conventional sensor	RMSE
1	1.110	1.105	0.003	1.150	1.145	0.003
2	3.741	3.727	0.009	1.210	1.197	0.009
3	6.471	6.456	0.009	0.980	0.970	0.007
4	9.410	9.399	0.007	0.831	0.827	0.002
5	12.220	12.214	0.004	0.811	0.798	0.008
6	14.212	14.208	0.001	0.370	0.362	0.005

The proposed *SubFRFDI* was applied to identify damage locations in the experimental frame. Figure 4 presents the *SubFRFDI* for damage scenarios 1–4. The highest corresponding *SubFRFDI* value indicated that the location of severest damage was on the first floor in damage scenarios 1–3 (Figs. 4(a)–16(c)). The *SubFRFDI* also identified damage on the third floor in damage scenario 4 (Fig. 4(d)). Figure 5 compares the damage indexes achieved by the proposed *SubFRFDI* and the *FRFCDI* for damage scenario 1. For comparison, the maximum values of *FRFCDI*　 and *SubFRFDI* were normalized to 1. The proposed approach for detecting damage locations performed superior to that of the FRF curvature method (Fig. 5).

5. CONCLUDING REMARKS

This work applied a novel substructure-based FRF approach with an Imote2.NET-based wireless SHM system to determine the locations of structural damage. Damage locations were identified using the novel *SubFRFDI*. Experimental studies were conducted to verify the performance of the proposed approach. The following conclusions are based on experimental results.

i. This work presents an easy-to-use development environment based on the .NET Micro Framework. Applications can be implemented efficiently under the .NET Micro Framework with a more user-friendly development environment. This accelerated development of SHM applications demonstrates the importance of the user-friendly development environment.

ii. Experimental analysis confirms the high quality of data collection by the proposed wireless sensing system. This reliable data-sensing and transmission protocol provided excellent data sensing and transmission quality for determining dynamic structural properties. In the experimental study, the proposed *SubFRFDI* located damage conveniently and accurately.
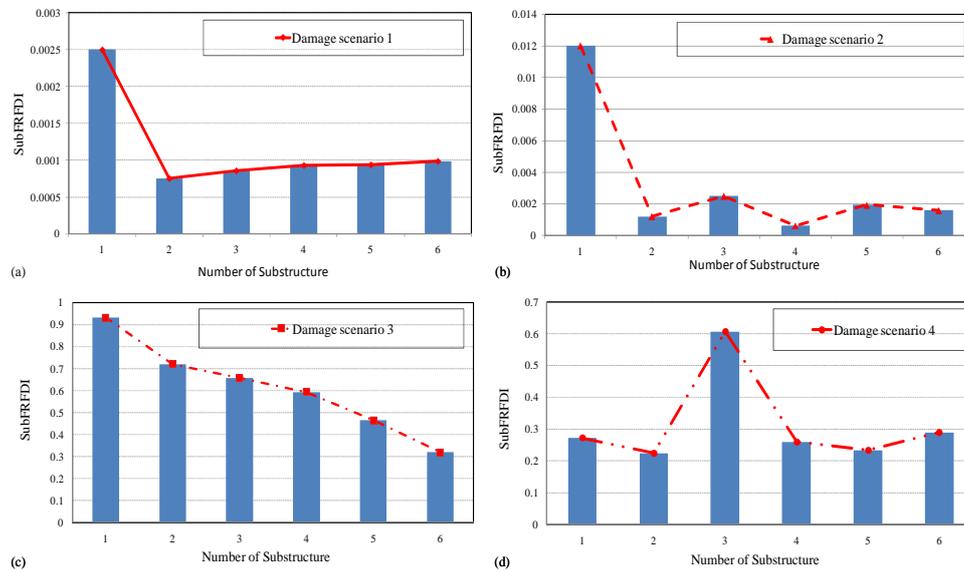

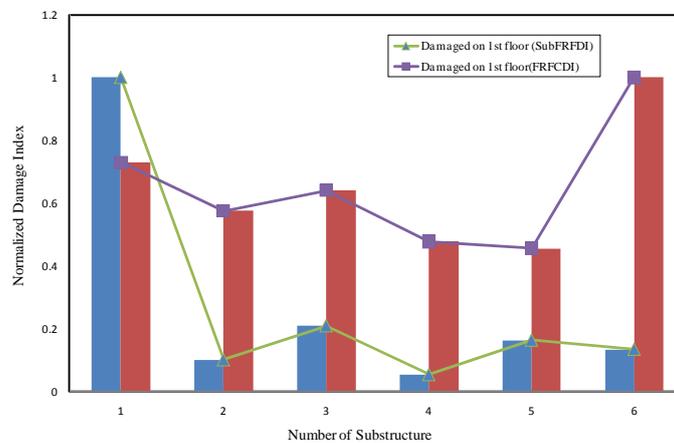**Figure 4.** The *SubFRFDI* for damage scenarios 1–4.

Figure 5. Comparison of the damage indexes obtained by the proposed *SubFRFDI* and the *FRFCDI* for damage scenario 1.

REFERENCES

Worden, K., Farrar,C.R., Haywood, J. and Todd, M. (2008). A review of nonlinear dynamics applications to structural health monitoring, *Struct. Control Hlth.* **15**, 540-567.

Sohn, H., Farrar, C.R., Hemez, F.M., Shunk, D.D., Stinemates, D.W., and Nadler, B.R. (2004). *A review of structural health monitoring literature: 1996-2001*, Los Alamos National Laboratory.

Cauberghe, B., Guillaume, P., Verboven, P., Vanlanduit, S., and Parloo, E. (2004). Frequency response function-based parameter identification from short data sequences, *Mech. Syst. Signal. Pr.* **18**, 1097-1116.

Celic, D. and Boltezar, M. (2008). Identification of the dynamic properties of joints using frequency-response functions, *J. Sound Vib.* **317**, 158-174.

Thyagarajan, S.K., Schulz, M.J., Pai, P.F., and Chung, J. (1998). Detecting structural damage using frequency response functions, *J. Sound Vib.* **210**, 162-170.

Lee, U., and Shin, J. (2002). A frequency response function-based structural damage identification method, *Comput. Struct.* **80**, 117-132.

Sampaio, R.P.C., Maia, N.M.M., and Silva, J.M.M. (1999). Damage detection using the frequency-response-function curvature method, *J. Sound Vib.* **226**, 1029-1042.

Maia, N.M.M., Silva, J.M.M., Almas, E.A.M., and Sampaio, R.P.C. (2003). Damage detection in structures: from mode shape to frequency response function methods, *Mech. Syst. Signal Pr.* **17** ,489-498.

Liu, X., Lieven, N.A.J., and Escamilla-Ambrosio, P.J. (2009). Frequency response function shape-based methods for structural damage localisation, *Mech. Syst. Signal Pr.* **23**, 1243-1259.

Ni, Y.Q., Zhou, X.T., and Ko, J.M. (2006). Experimental investigation of seismic damage identification using PCA-compressed frequency response functions and neural networks, *J. Sound Vib.* **290**, 242-263.

Furukawa, A., Otsuka, H., and Kiyono, J. (2006). Structural damage detection method using uncertain frequency response functions, *Comput.-Aided Civ. Inf.* **21**, 292-305.

Kanwar, V.S., Kwatra, N., Aggarwal, P., and Gambir, M.L. (2008). Health monitoring of RCC building model experimentally and its analytical validation, *Eng. Computation* **25**, 677-693.

Hsu, T.Y., and Loh, C.H. (2009). Damage detection using frequency response functions under ground excitation, *Proceedings of Sensors and Smart Structures Technologies for Civil, Mechanical, and Aerospace Systems*, San Diego, CA, USA.

Lynch, J.P. and Loh, K.J. (2006). A summary review of wireless sensors and sensor networks for structural health monitoring, *Shock and Vib. Dig.* **38**, 91-130.

Spencer Jr, B.F., Ruiz-Sandoval, M.E., and Kurata, N. (2004). Smart sensing technology: opportunities and challenges, *Struct. Control Hlth.* **11**, 349-368.

Nagayama, T., Spencer, B.F., and Rice, J.A. (2009). Autonomous decentralized structural health monitoring using smart sensors, *Struct. Control Hlth.* **16** , 842-859.

Rice, J.A., Mechitov, K., Sim, S.H., Nagayama, T., Jang, S., Kim, R., Spencer, B.F., Agha, G., and Fujino, Y. (2010). Flexible smart sensor framework for autonomous structural health monitoring, *Smart Struct. Syst.* **6**, 423-438.

Syed, Y., and Heidemann, J. (2006). Time synchronization for high latency acoustic networks, *Proceedings of IEEE Infocom*, Barcelona, Catalunya, Spain.

Ganeriwal, S., Kumar, R., and Srivastava. M. (2003). Timing-sync protocol for sensor networks, *Proceedings of 1st international conference on Embedded networked sensor systems*, Los Angeles, California, USA.

Wen, C.M., Hung, S.L., Huang, C.S., and Jan, J.C. (2007). Unsupervised fuzzy neural networks for damage detection of structures, *Struct. Control Hlth.* **14**, 144-161.

Allemang, R. J. (2003). The modal assurance criterion–twenty years of use and abuse, *Sound Vib.* **37**, 14-21.

Huang, C.S., Hung, S.L., Wen, C.M., and Tu, T.T. (2003). A neural network approach for structural identification and diagnosis of a building from seismic response data, *Earthquake Eng. Struc.* **32**, 187-206.